Titanium K-shell x-ray production from high velocity wire arrays implosions on the 20-MA Z accelerator

C. Deeney, C.A. Coverdale, M.R. Douglas, T.J. Nash,
R.B. Spielman, & K.W. Struve
Sandia National Laboratories, MS-1194
PO Box 5800
Albuquerque, N.M. 87185-1194

K.G. Whitney, J.W. Thornhill, J.P. Apruzese, R.C. Clark, & J. Davis
Plasma Physics Division
4555 Overlook Ave, SW
Naval Research Laboratory,
Washington D.C. 20375

F.N. Beg & J. Ruiz-Comacho
Plasma Physics Group
Imperial College, London, UK

Abstract

The advent of the 20-MA Z accelerator [R.B. Spielman, C. Deeney, G.A. Chandler, et al., Phys. Plasmas 5, 2105, (1997)] has enabled implosions of large diameter, high-wire-number arrays of titanium to begin testing Z-pinch K-shell scaling theories. The 2-cm long titanium arrays, which were mounted on a 40-mm diameter, produced between 75 ± 15 to 125 ± 20 kJ of K-shell x-rays. Mass scans indicate that, as predicted, higher velocity implosions in the series produced higher x-ray yields. Spectroscopic analyses indicate that these high velocity implosions achieved peak electron temperatures from 2.7 ± 0.1 to 3.2 ± 0.2 keV and obtained a K-shell emission mass participation of up to 12%.
PACS 52.25.Nr, 52.65.-y, 52.55.Ez, 52.50.Lp

cdeene@sandia.gov

DISCLAIMER

DISCLAIMER

Portions of this document may be illegible in electronic image products. Images are produced from the best available original document.

I. Introduction.

Z-pinches have been studied extensively as a source of x-rays between 0.1 and 3 keV for diverse applications.[1-8] Most of these applications have taken advantage of the efficiency of Z-pinches at producing x-rays at the low end of the range. Typical conversion efficiencies from stored electrical energy into x-rays vary from 20% for sub-keV emissions to 5 to 2% for 1 to 3 keV photon energies, respectively. For some applications, like radiation-material interactions and atomic physics measurements, photon energies above 4 keV are needed. However, the efficacy of Z-pinch x-ray sources to produce radiation above 4 keV has been limited by the ability of electrical drivers, at the less than 8 MA level, to uniformly implode sufficient mass, at high enough velocity to produce efficient excitation and ionization of high-lying ionization stages. For example, the 8-MA Saturn generator [9] has produced at most 10 kJ of titanium K-shell x-rays at 4.8 keV from a 25-mm-diameter 12-wire array, whereas the same generator can produce 40 kJ of argon K-shell x-rays at 3 keV from a 25-mm-diameter, argon gas puff.

The scaling of Z-pinches for higher energy K-shell photon sources has been considered theoretically[4,8,10,11] and is known to be a major challenge, primarily due to the demand for high temperatures, as well as, the high densities needed for the rapid thermalization of the implosion kinetic energy. This requirement for high temperatures and densities results in three equally important issues. First, the velocities needed to ionize into the K-shell of $Z=22$ and above exceed 60 cm/μs. To achieve these velocities with enough mass, high current generators are required, allowing large initial diameter Z-pinches to be conveniently used, but these loads can be susceptible to Rayleigh-Taylor (RT) [12] instability growth. Second, the need for high density plasmas demands good radial convergence, therefore very symmetric implosions. Finally, the radiation rates from the L-shell of elements above $Z=22$ are large and, in experiments to date, they result in sufficient energy losses, as the kinetic energy of the imploding shell is thermalizing, to prevent ionization into the K-

shell.[11] Of course, these issues are also coupled. For example, RT can broaden, and slow the imploding shell thereby reducing the on-axis thermalization rate, which in turn, allows the L-shell emissions to further slow the plasma heating before the K-shell ionization can occur. Unfortunately, Z-pinches at the 4 MA (Double-EAGLE [13]) to 8 MA level (Saturn [9]) are always going work to in an inefficient regime for atomic numbers greater than 20. As a result, for higher Z loads, only a small fraction of the load mass participates in K-shell emission, and consequently, these loads are sensitive to uniformity and stability issues. Moreover, the low masses that can be driven on these generators translate to low wire numbers, so not surprisingly, higher energy K-shell loads tested on these machines did not radiate well, and there was general pessimism about the potential efficiency of these higher atomic number pinches on even larger generators.

The experiments discussed in this paper were designed to investigate scaling issues as they relate to the production of titanium K-shell x-rays at 4.8 keV. These experiments are unique since they were performed at the 20 MA level on the Z accelerator at Sandia National Laboratories.[13] On Z, load masses between 800 and 2000 μg/cm can be imploded with high wire numbers (100 to 200) which have been shown to increase radiated x-ray powers due to improved pinch quality.[6,14,15] Z therefore provides the first opportunity to study a titanium K-shell radiation source in regimes where theory suggests that efficient x-ray production is possible,[10] and with masses where high wire number loads can be manufactured. Using the two smallest available pure titanium wires (20.3-μm and 25.4-μm diameter), arrays of 80 to 140 wires could be assembled, i.e. load masses from 1325 to 2060 μg/cm. These wire numbers give inter-wire separations of 1.6 to 1 mm. By cladding the titanium with nickel, it is possible to produce 15.2-μm diameter wires. In this case, the nickel accounts for about 15% of the wire mass. These thinner wires allow for increased wire number arrays, but at a cost, since the nickel enhances soft x-ray radiation losses.

In section II we will discuss the theory that guided the design of the titanium wire array experiments. We will present the experimental shot plan, and we will describe one dimensional, radiation-magnetohydrodynamic (MHD) calculations of titanium wire arrays to evaluate their performance on the 20-MA Z accelerator. In section III, we will describe the Z accelerator and the diagnostics. The yield, power and spectroscopy results from the titanium implosions are presented in Section IV. We make our conclusions and suggestions for future work in Section V.

II. Titanium Load Design for the 20-MA Z Accelerator.

The determination of the load parameters used in these experiments was guided by past experience with aluminum load designs on the Saturn and Double Eagle accelerators. Several factors must be taken into account in order to successfully scale from aluminum to titanium loads. First, the minimum energy requirements are higher for titanium than aluminum, but how much higher is yet to be determined. At a bare minimum, they are six times higher per atom, and L-shell radiation losses will increase this number. Second, a minimum amount of array mass is needed to achieve the densities on axis that are required for rapid kinetic energy thermalization and for efficient x-ray production. Third, a sufficiently large number of small diameter wires have to be used in order to guarantee a minimum implosion symmetry and stability.

The minimum energy requirements for aluminum have been determined from both past experimental and theoretical work. To rapidly ionize into the K-shell, one must achieve a rapid conversion of implosion kinetic energy into plasma thermal and ionization energies. For this conversion to terminate in the K-shell, each ion must carry a minimum kinetic energy, E_{min}, which is dependent on the atomic number, Z, of the load. E_{min} has been determined theoretically to scale as $E_{min} = 1.012 Z^{3.662}$ eV/ion. [8] For titanium, $Z = 22$ and $E_{min} = 84$ keV/ion. If an ion's kinetic energy can be converted entirely into stationary plasma energy with negligible losses from x-ray emission, then a minimal implosion velocity,

4

$(v_{imp})_{min}$ can be determined from the equation, $(1/2)m_i(v_{imp})^2_{min} = E_{min}$ (where m_i is the ion mass), which yields the value, 58 cm/μs for Ti. It is convenient to define the dimensionless energy, $\eta = (1/2)m_i v^2_{imp} / E_{min}$. The first requirement on titanium load design for the Z accelerator was that η be larger than 1.5 in order to allow for some of the L-shell radiation losses that were expected in these experiments. It was anticipated that η must, in fact, be larger than 2 to ensure a large K-shell mass participation fraction.[14] The experiments described in this paper tend to support this speculation.

The mass requirements for the titanium loads were also set by arguments based on the atomic number (Z), and by past experience with aluminum wire loads on Saturn. Early calculations of aluminum implosions with predominantly kinetic energy inputs and a fixed final implosion velocity [4] had shown a relatively sharply defined transition between two K-shell yield scaling regimes, an m^2 and an m regime, where m is the mass-per-length of the imploding aluminum plasma. The mass at which this transition occurs is termed the mass breakpoint, m_{BP}. It was found to be a function of η and simple arguments suggested that it scaled as $Z^{6.06}exp(20.6/Z^{0.9})$.[4] Subsequent calculations, [8,15] which varied the viscosity and heat conductivity in order to obtain phenomenological agreement with the measured parameters of the stagnated plasma, showed that the mass breakpoint was also a strong function of the implosion dynamics. The aluminum mass breakpoints calculated in Ref. 4 using classical transport coefficients are a factor of 6 less than those calculated in Ref. 8 using enhanced transport coefficients. The dependence of the mass breakpoint on dynamical factors such as may arise in the design of gas puff, small wire number, or large radius experiments makes it a somewhat idealized concept. However, the significance of the $m = m_{BP}(\eta)$ curve for aluminum experiments on Saturn [13] and in the calculations of Ref. 4 was that it defined the upper boundary of a region in (m, v_{imp}) space in which the efficient emission of K-shell x rays could be expected. The mass of the titanium loads was chosen by requiring that these loads fall in or close to this region.

The planned shots are listed in Table 1, and the pure titanium shots are displayed in Fig. 1 relative to the mass breakpoint and the $\eta = 2$ and 4 curves for titanium. In Table 1, we list the shot number, the array diameter (all 40 mm), the wire number, the wire diameter, and the array mass. In addition, we tabulate the kinetic energy, velocity and η as calculated from a circuit code coupled to a zero dimensional implosion model. The mass breakpoint curve, in Fig. 1, which is marked as "soft" is scaled from the mass breakpoint curves of Refs. 8 and 13. This curve was calculated based on comparisons of calculations to low wire number and gas puff experiments where the pinch quality was less than can now be achieved. This "soft" curve is shifted to higher masses by a factor of six from the mass breakpoint curve labeled as "hard". The latter curve was determined in reference 4 from one-dimensional calculations that employed classical transport coefficients, and it is plotted in Fig 1. for $\eta > 4$. These calculations produced pinches that were tight (sub-millimeter) with power pulses of 1 ns or less in duration. Since final pinch diameter is a function of wire number, the breakpoint curves that may be measured in an experiment using high wire numbers, may be expected to sit between these curves. For the low η regime ($\eta < 4$), Ref. 10 makes the point that it is of limited utility to quantify the breakpoint boundary because it depends too much on the type of experiment. In general though, this reference does show that in the low η regime, the mass breakpoint will occur at even large masses than those predicted by the "soft" curve. Moreover, the unquantified role of the L-shell radiation losses on the efficiency of the conversion of kinetic energy into x-rays in any experiment, introduces uncertainty into the required value of η.

Three points were considered in selecting the shots in Table 1: (a) the influence of plasma asymmetries and instabilities was minimized by fixing the array diameter at 40 mm; (b) the placement of the mass breakpoint curve was tested by carrying out a mass scan using 20.3-μm diameter wires; and (c) the effects of pinch quality were investigated by carrying out a wire number scan from 80 to 160 wires and by making a comparison of similar arrays with and

6

without nickel cladding. Since reductions in the array mass lead to higher implosion velocities, they also move the implosions closer to the mass breakpoint curve as shown in Fig. 1. It was expected that the smallest mass show would produce the largest K-shell yield because of its close proximity to the mass breakpoint curve and because this curve also defines the locus of shots with the highest K-shell yields per given energy input.[13] For future interest, the two inverted triangles that are located on the $\eta = 4$ curve show the masses needed to achieve this η value on the Z accelerator. A mass of 0.55 mg/cm is required for a 40 mm diameter array, while a higher mass of 0.75 mg/cm can be imploded from a 50 mm diameter. To maintain implosion quality from a 50 mm diameter, more thinner wires would be very desirable.

III. The 20-MA Z Accelerator and Diagnostics.

The Z accelerator [16] at Sandia National Laboratories is a 36 module pulsed power generator that stores 11.5 MJ in its Marx banks. When fired, the Marxes erect producing a 5 MV pulse, and discharge in 1.2 μs into water intermediate energy storage capacitors (IES). The gas output switches of the IESs are laser-triggered with a first-to-last spread of 15 ns. Upon triggering, the IESs pulse charge 36 pulse forming lines (PFLs) with self-breaking water output switches. The PFLs generate a 50 TW, 100 ns duration electrical pulse, at the insulator stack, which delivers 3 MJ of electrical energy into the vacuum region. The total peak current in the four magnetically insulated transmission lines (MITLs) is 20 MA. A double post hole convolute combines the currents from the four MITLs together just down stream of the load region. Due to electron losses in the convolute, the load currents are in the range of 16 to 18 MA. A detailed circuit model exists for Z and it is employed with a zero-dimensional implosion model to calculate kinetic energies and collapse velocities for a defined compression ratio.

To quantify and characterize the x-ray emissions from the Z-pinch, an extensive suite of x-ray diagnostics are fielded on each shot. The 0.2 to 2.5 keV x-rays are

7

measured with a five channel x-ray diode (XRD) array.[17] A six channel array of filtered diamond photoconducting detectors are employed to measure the x-rays in the 0.8 to 10 keV range.[18]   Lastly, two identical, unfiltered, 1-μm-thick nickel bolometers are used to measure the total radiated x-ray and power.[19]

The dynamics of the pinched plasma are recorded by a nine-frame time-resolved pinhole camera with 100 ps, 100 μm temporal and spatial resolution. The x-ray spectra between 1 and 7 keV are measured using a KAP (potassium acid phathalate) time-integrating spectrometer oriented for 1-mm radial resolution, and a 7-frame 2-ns gated time-resolved spectrometer. A time-integrating MICA crystal spectrograph, operating in third order, with 1-mm axial resolution, and a 2-ns gated time-resolving third order MICA spectrometer measure the titanium K-shell emissions.

IV. Experimental Results.

In Table 2, we summarize the results from the series of shots described in Table 1. Before discussing the trends in the data, it is useful to examine the individual shot data. The measured MITL and load currents, total power, kilo-electron-volt power and K-shell power are shown in Figure 2 for shot Z302; this is a 40-mm-diameter array with 90 titanium wires of 20.3 μm diameter as listed in Table 1. Figure 2(a) depicts the total and kilo-electron-volt x-ray powers overlayed with the MITL and load currents. The total power peaked at 63±10 TW with a FWHM of 13-ns, corresponding to an energy in the main Gaussian pulse of 800 kJ, while the total radiated energy was measured to be 1.1±0.2 MJ. The total x-ray power had an extrapolated start at 97 ns and peaked at 109 ns. The circuit model coupled to a zero dimensional implosion model would suggest a kinetic energy of 0.98 MJ and implosion velocity of 83 cm/μs for a 14:1 compression ratio. Figure 2(b) shows the total, kilo-electron-volt and K-shell powers on an expanded timescale. The kilovolt power, pulsewidth and yield were measured

to be 20±2 TW, 12.6 ns and 295±40 kJ, while the K-shell yield was 125±25 kJ produced in a 12.4 ns FWHM, 7.5±1.0 TW power pulse.

The magnitude and FWHM of the measured total x-ray power from the titanium Z-pinches illustrate one of the important differences between a sub-kilo-electron-volt and a super-kilo-electron-volt x-ray source. The titanium pinched plasma was not as good a total radiator as 240-wire, 40-mm-diameter tungsten arrays on Z, which produce 200 TW, 6.5 ns FWHM power pulses.[16] This is due to many effects pertaining to the ionization dynamics, opacities and pinch quality. Indeed, as shown in Figure 3 (and Table 2), the titanium wire arrays produced approximately 3.0 mm diameter pinches, whereas a 240 wire tungsten array have pinch diameters of 1.5 mm. The total energy from these titanium pinches is also lower than the 1.6 to 1.8 MJ radiated by the tungsten arrays. The pinch energetics, however, is similar in one respect to the energetics observed in tungsten pinches, that is, the total energy exceeds the kinetic energy calculated even with a 20:1 compression ratio, and the peak x-ray power occurs as the current is falling, not at the minimum in the current. Peterson *et al* [20] and Thornhill *et al* [10] have suggested that the total radiated energy is fed by thermalization of the kinetic energy, by on-axis pdV work and by some ohmic heating. The lower total yields from titanium are due in part to its lower sub-keV radiation rate, which causes a decrease in the radial convergence and hence reduces the pdV contributions. Calculations are underway to study these energy issues. Another issue to be investigated in future calculations and experiments, is peaking of the kilo-electron-volt and K-shell powers after the peak in the total power pulse, which is suggestive of an ionization lag that is undesirable for efficient high energy x-ray production.

The magnitudes of the kilo-electron-volt and K-shell yields and powers that were observed in these experiments are very encouraging. As seen in Figure 4, they indicate that the Li- and Be-like stages of titanium, including the recombination continuum, are copious radiators. Indeed, the titanium kilo-electron-volt yield is comparable to the highest aluminum K-shell yields seen on

9

Z of slightly under 300 kJ. The ability of these mid-Z elements to radiate high energy K-shell photons while producing sizable yields from their L-shells make them very useful for applications requiring broad spectral x-ray sources.

The time-integrated K-shell spectrum in Fig 4(b) indicates that portions of the titanium plasma are ionized into both the He- and H-like stages. From the ratio of the Lyman-alpha to helium-alpha lines, the measured K-shell power and pinch size, the electron temperature, ion density and K-shell mass fraction can be estimated following Coulter, *et al* [21] and Apruzese, *et al.*.[22] Our spectroscopic analyses indicate that the K-shell emitting plasma reached an electron temperature of 3000 eV, an ion density of 3×10^{19} cm^{-3}, and a K-shell mass fraction of 12%. The fact that these implosions achieved the predicted high electron temperatures indicates that the limiting factors on K-shell yield were the densities, the mass fractions, and L-shell losses.

In the next sections, we will describe the trends observed as the initial array mass, wire number and, in a limited way, wire material were changed to study the variations in yields, powers and plasma parameter. All the relevant data are tabulated in Table 2.

A. Mass Scan.

By varying the mass of the array at a fixed diameter, the implosion time is changed without going to larger diameter arrays. This was a necessary first step with titanium since the limited available wire sizes would not allow for sufficient wires to hold the wire gap constant or small during an initial radius scan.[23-25] A constant-diameter, mass scan does mean that the kinetic energy coupling to the generator does reduce as the implosion time is decreased; specifically, the calculated kinetic energy decreases from 1.10 to 0.98 MJ over the range of implosion times shown in Figure 5. Figure 5(a) shows the measured total yield indeed decreased as the implosion time decreased, however, the K-shell yields increased for the shorter implosion

10

times. Shot Z67, however, a 40-mm array with the 80, 25.4 μm wires radiated the same total energy as a 110-wire array with 20.3 μm wires which had the most similar mass. The K-shell yield from Z67 was down and will be discussed in Sec. IV(B).

The zero-dimensional implosion model coupled to a circuit model of Z estimated velocities of 74, 76, 80 and 83 cm/μs, as the array mass was lowered and the implosion time was decreased. These velocities were used to make the η estimates for Fig. 5(b). Using Figure 5(b), we see that the K-shell mass fraction (which is determined from the spectra) and the ratio of the K-shell yield to total yield both increased as η value increased. The electron temperatures, see Table 2, indicate that the electron temperature did not increase significantly as η increased in the plasma regions of the titanium plasmas that were emitting K-shell x-rays. We deduce, therefore, that the higher η values led to faster ionization, less L-shell losses, and more of the mass being ionized into the K-shell. In the efficient regime, that is sufficiently high mass pinches, this increase in K-shell mass fraction would be expected, and has been observed with aluminum pinches.[14] How the L-shell losses determine the K-shell mass fractions, and how they are influenced by the temperature gradients formed during the stagnation of the pinch are subjects of experimental [26,27] and theoretical studies.[28] Detailed radiation-MHD calculations on how to control these factors are planned.

The consequence of the relatively low mass fractions can be seen in Figure 6, where the measured yields are compared to yields obtained from one-dimensional radiation-MHD calculations in ref. 10. The calculated curves are for three η^* values, and a mass-squared dependency is shown for reference. The quantity η^* is defined similarly to η, but rather the total energy per ion from kinetic, pdV and ohmic heating is normalized to the E_{min}. Normally, η^* will be larger than η. As the mass is increased in the calculations, the yield increases as mass-squared for low masses and then gradually transitions to scaling less

11

strongly with mass above 2000 µg/cm. Moreover, in the calculations, as the η^* value is increased, the yield also increases. Ideally, the measured yields for shots with η between 1.6 and 2.1 would have been expected to produce yields in the region of the curves for η^* between 2 and 3, i.e. about 100 kJ/cm. The measured yields for these parameters are 60 kJ/cm. In part, this difference is due to the lower K-shell mass fractions observed experimentally than those calculated. Clearly, increasing the mass fraction and hence the K-shell conversion efficiency is an important goal, which can best be achieved via larger η values, and/or improved implosion uniformity.

B. Wire Number Scan and the use of nickel cladding.

The x-ray power from Z-pinches is known to increase with increased wire number, [6,25] due to the formation of tighter, higher density pinches. In addition, experiments with argon gas puffs have also shown increased K-shell yields, as well as powers, with better implosion uniformity and compression.[29] Consequently, we explored the use of increased wire number to increase the titanium K-shell powers and yields by improving pinch quality.

In Figure 7, the measured FWHMs for the total and K-shell powers are plotted versus the inter-wire gap for the 40-mm arrays with masses of 1410 to 1840 µg/cm. The open symbols represent the data from the nickel-clad wires, which were employed to get to the thinner wire sizes. As has been seen with aluminum [15] and tungsten,[6] the pulsewidths decrease as the inter-wire gap decreases, or the wire number increases. As one might expect, due to the sensitivity of the K-shell emissions to density and to the additional heating mechanisms that contribute to the total powers, the K-shell power pulse narrows faster than the total power pulse. Apparently, we can also infer from Figure 7, that the nickel cladding did not significantly alter the implosion dynamics, since the nearly equivalent inter-wire gap shots with 20.3-µm-diam. titanium and nickel-clad titanium wires produced very similar pulsewidths. Before these

12

nickel clad wires were employed on Z, single wire explosions experiemnts were performed at Imperial College of the pure and clad wires at a rate of rise of current, i.e. 2.3 kA/ns per wire, similar to what they would be subjected to in a Z shot. Schlieren diagnostics indicated that the expansion of the nickel-clad titanium wire was more uniform, but slower than the pure titanium wire. Consequently, we believed that the cladding should not have adversely affected the implosion dynamics; this was borne out by the Z shots.

Before discussing the measured effects of wire number on the K-shell yields, it must be noted that the presence of the nickel did significantly alter the L-shell radiation rates from the pinches. From Table 2, it can be seen that nickel shot, Z313, produced 14% more total power, 20% more total yield, and 48% more 1 to 4 keV x-rays than the equivalent pure titanium shots Z119 and Z302. Consequently, Z313 produced 90 kJ of titanium K-shell x-rays rather than the 120±25 kJ produced by Z119 and Z302. This drop due to the nickel cladding is evident in Figure 8, where the measured K-shell yields are plotted versus inter-wire gap. From Figure 8, it can be seen for the pure titanium, and separately for the nickel clad shots, that the K-shell yield increased with decreased inter-wire gap. If the nickel clad data is scaled to compensate for the reduction compared to pure titanium, the data would suggest that the yield could have increased by 60% by increasing the wire number from 80 to 160 wires.

By comparing the plasma parameters in Table 2 inferred from the spectra of the pure titanium, we see that the increased wire number produced a 60% increase in mass fraction. The nickel clad data also showed increases in the same parameters when the wire number was increased; specifically, a 15% increase in density and a 20% increase in mass fraction. Based on these results, we will explore other cladding techniques that maximize the wire number while minimizing the impact of L-shell radiation losses. Hopefully, this will allow us to fully benefit from the thinner wires in terms of higher absolute yields. However nickel cladding does allow 15.2-µm-diam. wires to be fabricated, with which to perform radius scaling experiments in the future.

V. Conclusions and Future Work.

The first titanium experiments performed on Z have confirmed some of the key aspects of z-pinch scaling, and have also provided indications of how the higher photon energy K-shell emissions can be further enhanced. Firstly, they have shown that large K-shell yields, with $h\nu > 4$ keV, can indeed be produced by operating near the theoretically predicted efficient regime, using high-wire-number arrays that are more representative of the initial conditions employed in the one-dimensional calculations. Secondly, as η increased, the L-shell losses became relatively less and the fraction of the plasma emitting from the K-shell increased. Moreover, only a small increase in electron temperature is observed. This trend confirms previous measurements with aluminum pinches, [23] and again is expected behavior in the efficient regime. However, the data is still to sparse to determine the exact manner in which the L-shell radiation losses determine a minimum η value. Thirdly, the L-shell radiation losses from these titanium pinches are sizable, with hundreds of kilo-joules being emitted above 1 keV. In principle, if more wires are used, plasma uniformity will be increased and consequently a more rapid rate of kinetic energy thermalization will occur. This should preferentially increase the K-shell power relative to the L-shell loss rate. However, the effects of improved symmetry will be offset if the increased wire number is obtained by using materials that are better L-shell radiators than titanium.

The data from these experiments are very comprehensive. Future analyses will be needed to quantify the radlially-resolved (but time-integrated) and the time-resolved kilo-electron-volt and K-shell spectra to compare to radiation MHD calculations. This process will allow us to determine the time history of the heating and the temperature gradients. By using thinner clad titanium wires, we will be able to perform radius scan experiments in the future with improved array uniformity for higher η values. Future experiments might provided further

14

increases in yield if cladding techniques with metals that have lower atomic numbers than titanium can be developed.

References.

1. N. R. Pereira and J. Davis, J. Appl. Phys. **64**, R1 (1988).

2. J. L. Porter, R. B. Spielman, M. K. Matzen, *et al*, Phys. Rev. Lett. **68**, 796 (1992).

3. V.P. Smirnov, Plasma Phys. Controlled Fusion **33**, 1697, (1991)

4. K. G. Whitney, J. W. Thornhill, J. P. Apruzese, and J. Davis, J. Appl. Phys. 6, 1725 (1990).

5. J. W. Thornhill, K. G. Whitney, and J. Davis, J. Quant. Spectrosc. Radiat. Transfer **44**, 251 (1990).

6. C. Deeney, T.J. Nash, R.B. Spielman, *et al.*, Phys. Rev. E **56**, 5945, (1997).

7. P.T. Springer, K.L. Wong, C.A. Iglesias, *et al*, J. Quant. Spectrosc. Radiat. Transfer **58**, 927, (1997).

8. J. W. Thornhill, K. G. Whitney, C. Deeney, and P. D. LePell, Phys. Plasmas **1**, 321 (1994).

9. R. B. Spielman, R. J. Dukart, D. L. Hanson, B. A. Hammel, W. W. Hsing, M. K. Matzen, and J. L. Porter, ``Dense Z pinches, Second International Conference'' ed. by N. R. Pereira, J. Davis, and N. Rostoker, AIP Conference Proc. **195**, 3 (1989).

10. J.W. Thornhill, K.G. Whitney, J. Davis, and J.P. Apruzese, J. Appl. Phys. **80**, 710, (1996).

11. J. Davis, J.L. Giuliani, and M. Mulbrandon, Phys. Plasmas **2**, 1766, (1995).

12. T.W. Hussey, N.F. Roderick, U. Shumlak, R.B. Spielman and C. Deeney, Phys. Plasmas **2**, 2055, (1995).

13. K. G. Whitney, J. W. Thornhill, J. L. Giuliani, Jr., J. Davis, L.A. Miles, E.E. Nolting, V.L. Kenyon, W.A. Spicer, J.A. Draper, C.R. Parsons, P. Dang, R.B. Spielman, T.J. Nash, J.S. McGurn, L.E. Ruggles, C. Deeney, R.R. Prasad and L. Warren, Phys. Rev. E **50**, 2166 (1994).

14. C. Deeney, T.J. Nash, R.B. Spielman, et al, Phys. Plasmas **5**, 2431, (1998).

15. K. G. Whitney, J. W. Thornhill, J. P. Apruzese, et al., *Phys. of Plasmas*, **2**, 2590 (1995)

16. R.B. Spielman, C. Deeney, G.A. Chandler, *et al*, Phys.Plasmas **5**, 2105, (1998).

17. G.A. Chandler, C. Deeney, M. Cuneo, *et al*, Rev. Sci. Instrum. **70**, January, (1999).

18. R.B. Spielman, Rev. Sci. Instrum., **66**, 867, (1995).

19. R.B. Spielman, C. Deeney, J. McGurn, *et al*, accepted for Rev. Sci. Instrum. **70**, January, (1999).

20. D.L Peterson, R.L. Bowers, K.D. McLenithan, C. Deeney, G.A. Chandler, R.B. Spielman, M.K. Matzen, and N.F. Roderick, Phys. Plasmas **5**, 3302, (1998).

21. M.C. Coulter, K.G. Whitney and J.W.Thornhill, J. Quant. Spectrosc. Radiat. Transfer **44**, 443 (1990).

22. J. P. Apruzese, K. G. Whitney, J. Davis, and P. C. Kepple, J. Quant. Spectrosc. Radiat. Transfer **57**, 41, (1997).

23. C. Deeney et al, Bull. Am. Phys. Soc. **42**, 2069, (1997).

24. T.W.L. Sanford, R.C. Mock, R.B. Spielman, D.L. Peterson, D. Mosher, and N.F. Roderick, Phys. Plasmas **5**, 3755, (1998).

25. T. W. L. Sanford, G. O. Allshouse, B. M. Marder, *et al*, Phys. Rev. Lett. **77**, p5063, (1996).

26. C. Deeney, P. D. Lepell, B. H. Failor, S. L. Wong, J. P. Apruzese, K. G. Whitney, J. W. Thornhill, J. Davis, E. Yadlowsky, R. C. Hazelton, J. J. Moschella, T. Nash, and N. Loter, Phys. Rev. E **51**, 4823 (1995).

27. J.P. Apruzese, J.W. Thornhill, K.G. Whitney, et al, IEEE Trans. On Plasma Sci. 26, 1185, (1998).

28. J.P. Apruzese, et al, accepted for Phys. Plasmas, (1999).

29. C. Deeney, P.D. LePell, F.L. Cochran, M.C. Coultter, K.G. Whitney, and J. Davis, Phys Fluids B **5**, 992 (1993)

Table 1. Z shot parameters for the titanium wire array implosions.

Shot	Element	Array Diam. (mm)	Wire No.	Wire Diam. (μm)	Mass (μg/cm)	Kinetic Energy (kJ)	Velocity (cm/μs)	η
Mass and Wire number scan								
Z67	Ti	40	80	25.4	1840	1100	76	1.7
Z87	Ti	40	140	20.3	2060	1100	74	1.6
Z88	Ti	40	110	20.3	1620	1000	80	1.9
Z119	Ti	40	90	20.3	1320	975	83	2.1
Nickel cladding and wire number scan								
Z302	Ti	40	96	20.3	1413	980	83	2.1
Z313	Ti_Ni	40	90	20.3	1429	980	83	2.1
Z311	Ti_Ni	40	160	15.2	1429	980	83	2.1

Table 2. The measured yields, pulsewidths, and plasma parameters.

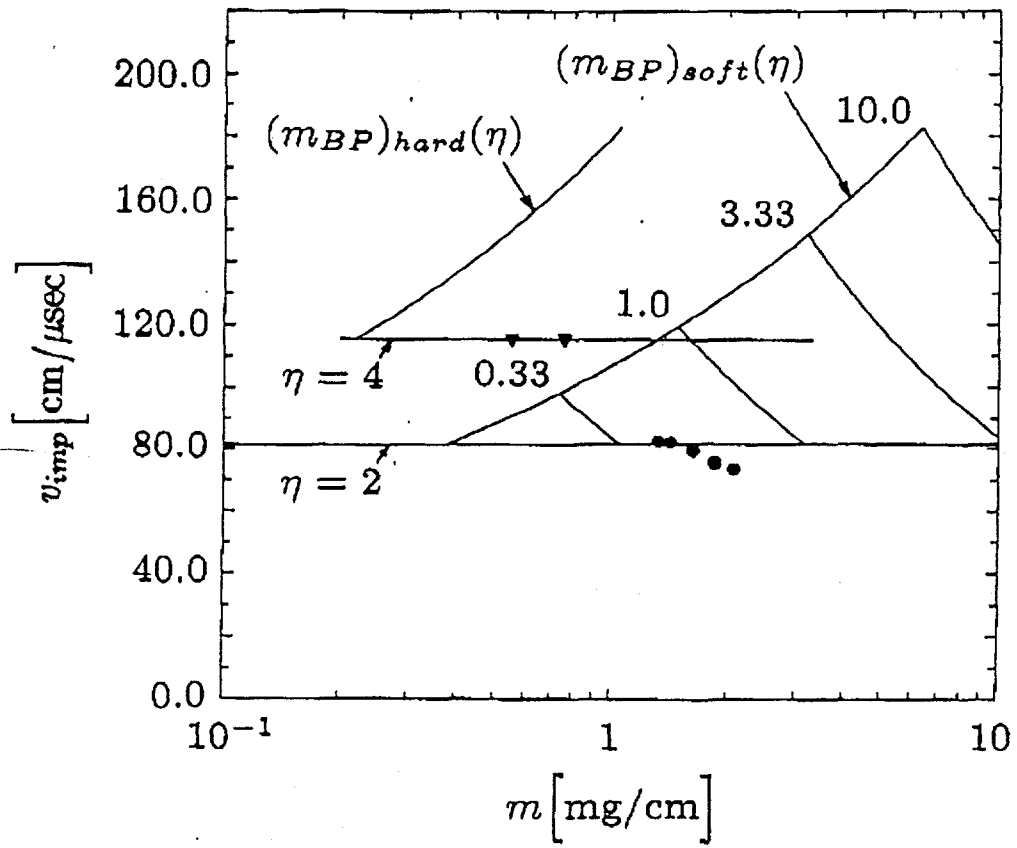| Shot	m (µg/cm)	Diam (mm)	Total Yield (kJ)	Total FWHM (ns)	KeV Yield (kJ)	K-shell Yield (kJ)	K-shell FWHM (ns)	Te (eV)	Ni x10^{19} (cm-^{3})	mk/m (%)
Z67	1840	2.8	1200	18.0	N/A	75	18.0	2700	2.0	5
Z87	2060	2.8	1250	16.4	N/A	92	10.0	2700	2.3	5
Z88	1620	2.8	1150	12.0	N/A	100	10.0	2700	2.5	8
Z119	1320	2.8	N/A	12.0	300	125	11.0	3000	3.0	12
Z302	1413	3.0	1060	13.8	295	120	12.4	N/A	N/A	N/A
Z313	1429	2.9	1280	13.0	350	90	11.0	2800	2.8	10
Z311	1429	2.5	1340	9.8	390	110	6.0	3200	3.2	12

Figure Captions.

Figure 1. A schematic of a region in mass and velocity space defined by an $\eta = 2$ curve and the locus of points which define the mass-breakpoint, for soft and hard implosion calculations, as a function of η. The dots denote the location, in this phase space, of the shots in Table 1. For reference, lines of constant kinetic energy are shown for 0.33, 1, 3.33, and 10 MJ/cm.

Figure 2. The measured currents and x-ray powers from Snot Z302, a 40-mm diameter, 96-wire array with 20.3-μm-diameter titanium wires. In (a), the load (solid) and MITL (dashed) currents are shown, along with the total power (solid) and kilo-electron-volt (dashed) x-ray powers. The total (solid), kilo-electron-volt (dashed) and K-shell (dash-dot) x-ray powers are shown in (b) with an expanded time scale.

Figure 3. An example of time-resolved pinhole images from Z313.

Figure 4. Examples of (a) a titanium spectrum from 1 to 6 keV, and (b) .a detailed K-shell spectrum.

Figure 5. (a) A plot of the measured total (circles) and K-shell (triangles) x-ray yields versus the implosion time for 40-mm-diameter arrays composed of 20.3-μm-diameter titanium wires. The open circles and triangles are for Z67 the array with 25.4-μm-diameter wires. In (b), the measured K-shell mass fraction (circles) and the ratio of K-shell to total yields (squares) are plotted versus the dimensionless kinetic energy per ion, η.

Figure 6.   A comparison of the measured K-shell yields to those predicted by one-dimensional radiation-MHD calculations taken from Ref. 10. The η values for the experimental points are marked next to the plot symbols.

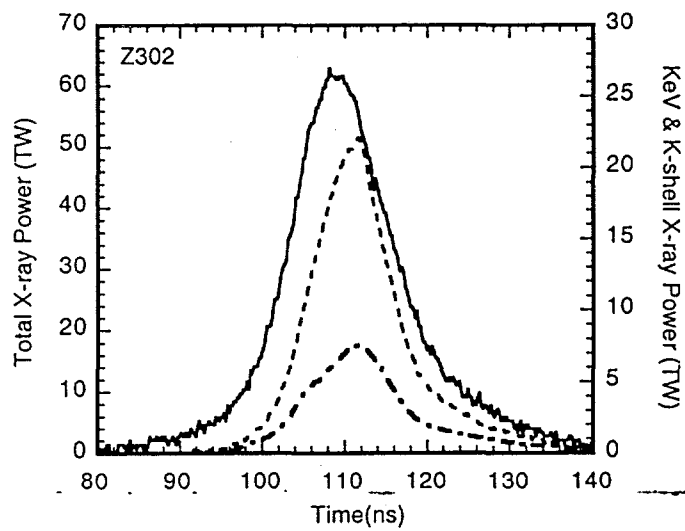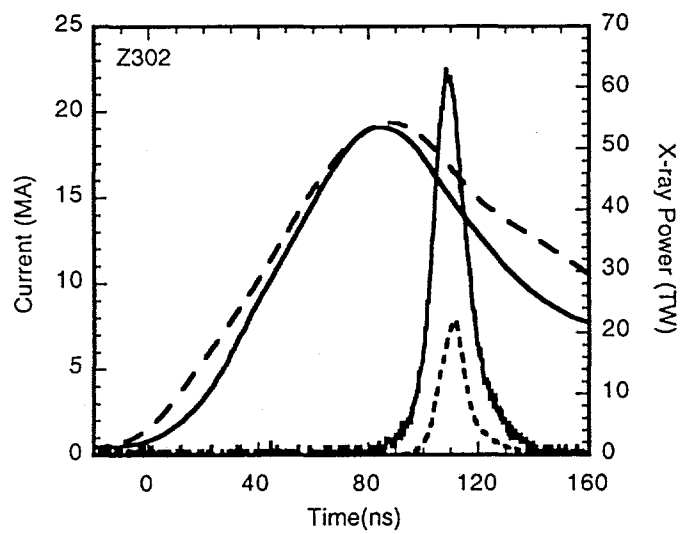Figure 7.   The measured FWHM of the total power(circles) and K-shell power (triangles) both decrease as the inter wire gap is decreased, that is the wire number is increased. The open symbols are for shots where nickel cladding was employed.
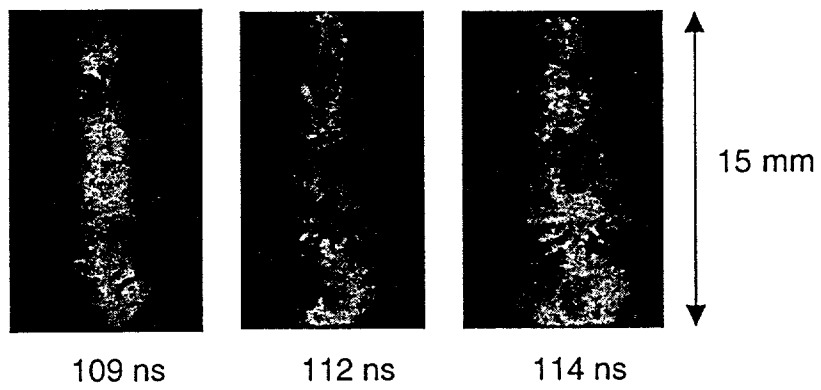
Figure 8.   The titanium K-shell yields versus inter-wire gap. The open symbols are for the nickel-clad wire arrays.
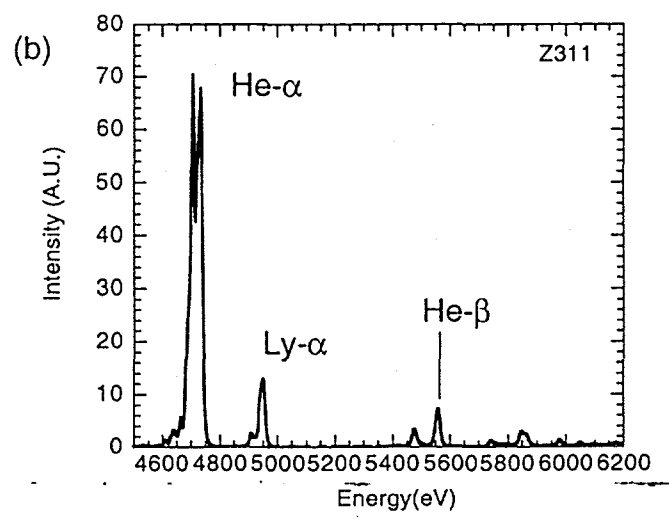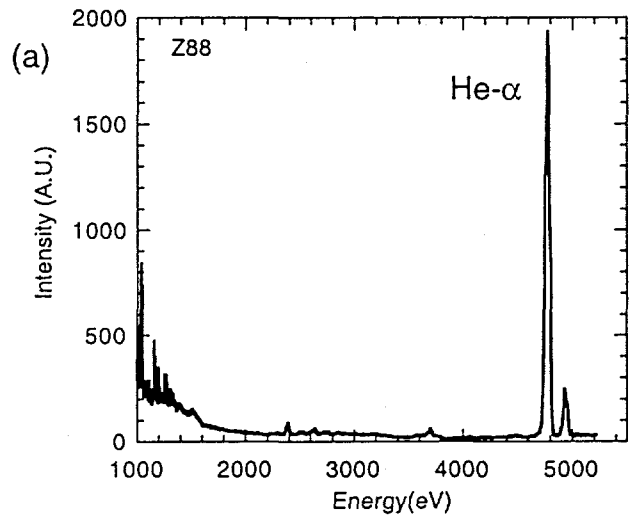
C. Deeney, et. al.   Fig. 1
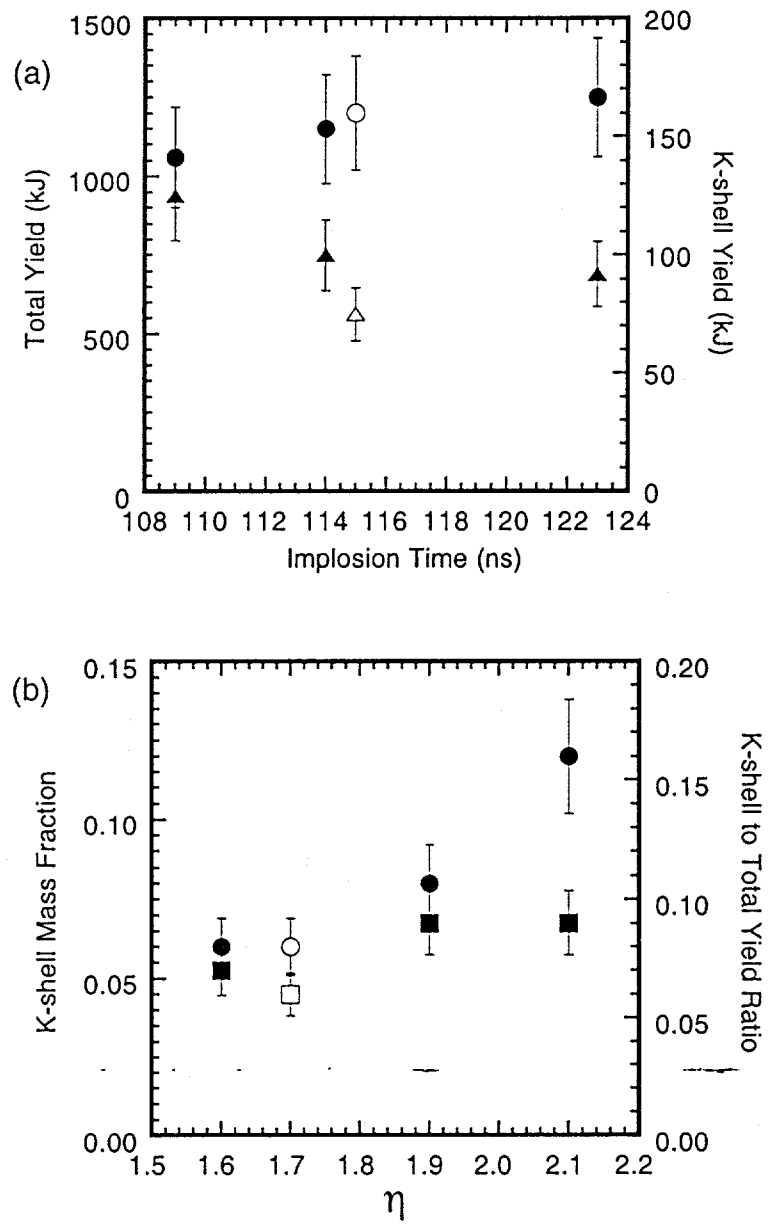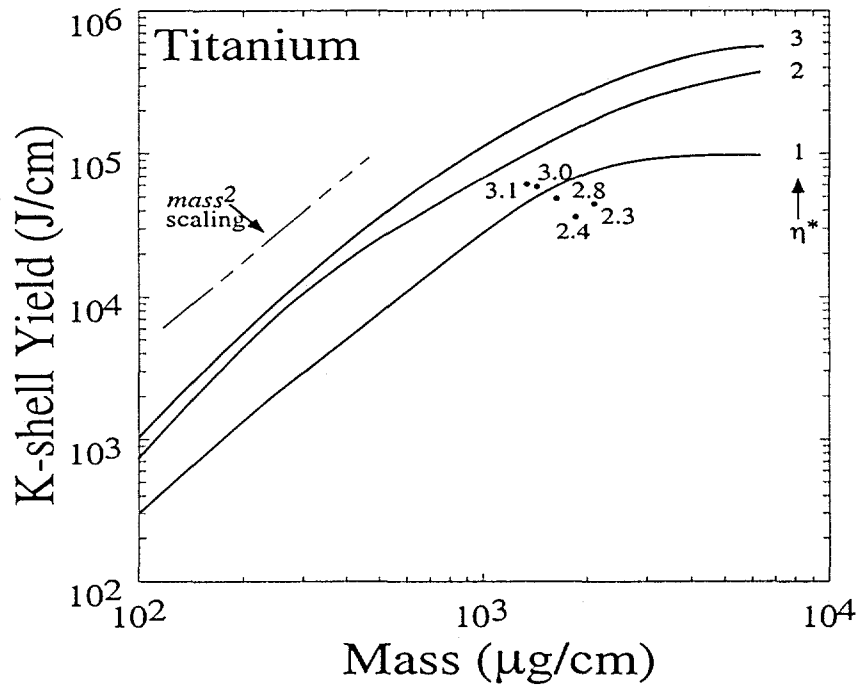
C. Deeney et al   Fig.   2

109 ns   112 ns   114 ns

15 mm

C. Deeney et al   Fig.   3

(a) Z88
He-α

(b) Z311
He-α
Ly-α
He-β

C. Deeney et al   Fig.   4

(a)

(b)

C. Deeney et al   Fig.   5

Titanium

mass² scaling

3.1 3.0
2.8
2.4 2.3

η*

3
2
1

K-shell Yield (J/cm)

Mass (μg/cm)

Note - these η values will be changed!!

C. Deeney et al   Fig.   **6**

C. Deeney et al   Fig.   7

C. Deeney et al   Fig.   8